Journal of Inorganic Biochemistry 199 (2019) 110760

Contents lists available at ScienceDirect

Journal of Inorganic Biochemistry

journal homepage: www.elsevier.com/locate/jinorgbio

Copper ion vs copper metal–organic framework catalyzed NO release from bioavailable *S*-Nitrosoglutathione en route to biomedical applications: Direct ^{1}H NMR monitoring in water allowing identification of the distinct, true reaction stoichiometries and thiol dependencies

Robert R. Tuttle[a], Heather N. Rubin[a], Christopher D. Rithner[a], Richard G. Finke[a], Melissa M. Reynolds[a,b,c,*]

[a] Department of Chemistry, Colorado State University, Fort Collins, CO 80523, United States
[b] School of Biomedical Engineering, Colorado State University, Fort Collins, CO 80523, United States
[c] Department of Chemical & Biological Engineering, Colorado State University, Fort Collins, CO 80523, United States

ARTICLE INFO

Keywords:
^{1}H NMR
MOF
Nitric oxide
Catalysis
Stoichiometry
S-Nitrosoglutathione

ABSTRACT

Copper containing compounds catalyze decomposition of *S*-Nitrosoglutathione (GSNO) in the presence of glutathione (GSH) yielding glutathione disulfide (GSSG) and nitric oxide (NO). Extended NO generation from an endogenous source is medically desirable to achieve vasodilation, reduction in biofilms on medical devices, and antibacterial activity. Homogeneous and heterogeneous copper species catalyze release of NO from endogenous GSNO. One heterogeneous catalyst used for GSNO decomposition in blood plasma is the metal-organic framework (MOF), $H_3[(Cu_4Cl)_3$-$(BTTri)_8$, H_3BTTri = 1,3,5-tris(^{1}H-1,2,3-triazol-5-yl) benzene] (CuBTTri). Fundamental questions about these systems remain unanswered, despite their use in biomedical applications, in part because no method previously existed for simultaneous tracking of [GSNO], [GSH], and [GSSG] in water. Tracking these reactions in water is a necessary step towards study in biological media (blood is approximately 80% water) where NO release systems must operate. Even the balanced stoichiometry remains unknown for copper-ion and CuBTTri catalyzed GSNO decomposition. Herein, we report a direct ^{1}H NMR method which: simultaneously monitors [GSNO], [GSH], and [GSSG] in water; provides the experimentally determined stoichiometry for copper-ion vs CuBTTri catalyzed GSNO decomposition; reveals that the CuBTTri-catalyzed reaction reaches 10% GSNO decomposition (16 h) without added GSH, yet the copper-ion catalyzed reaction reaches 100% GSNO decomposition (16 h) without added GSH; and shows 100% GSNO decomposition upon addition of stoichiometric GSH to the CuBTTri catalyzed reaction. These observations provide evidence that copper-ion and CuBTTri catalyzed GSNO decomposition in water operate through different reaction mechanisms, the details of which can now be probed by ^{1}H NMR kinetics and other needed studies.

1. Introduction

Generation of NO carries great importance in medicine as NO is a vital signaling molecule in the human nervous [2,3], immune [4,5], and cardiovascular systems [6,7], as well as an effective antibacterial agent [8,9]. *S*-Nitrosothiols (RSNOs) [1] such as *S*-Nitrosoglutathione (GSNO) have attracted attention as endogenous sources of NO, GSNO being of particular importance due to its presence in human blood [10,11]. One equivalent of NO is known to form per equivalent of GSNO decomposed along with disulfide (RSSR) formation [12,13]. Long-term NO generation for biomedical applications is desirable [14,15] and can be achieved by pairing an endogenous NO source such as GSNO with a catalyst that induces GSNO decomposition *in water* rather than organic solvents where RSNO decompositions have been studied. For example, the study of homogeneous copper model complexes in organic solvents such as dichloromethane [21] and toluene [24] have appeared. Relevant here is that water is an important solvent for RSNO studies given that blood is ca. 80% water, and blood is where NO release is important for applications under development [16].

Copper-containing compounds are an important family of RSNO decomposition catalysts. Solvated Cu^{2+} is the most commonly studied copper ion pre-catalyst for RSNO conversion [17]. Reduction of Cu^{2+} to

* Corresponding author at: Department of Chemistry, Colorado State University, Fort Collins, CO 80523, United States.
E-mail address: melissa.reynolds@colostate.edu (M.M. Reynolds).

https://doi.org/10.1016/j.jinorgbio.2019.110760
Received 7 June 2019; Received in revised form 24 June 2019; Accepted 7 July 2019
Available online 16 July 2019
0162-0134/

Cu^{+} is hypothesized as a necessary step in the reaction mechanism [18]. Thiols (RSH) have been used as reducing agents at sub stoichiometric concentrations to initiate the catalytic cycle and increase the rate of copper ion catalyzed RSNO decomposition [19]. Thiols are thought to play a dual role in these systems, as reducing agents to generate Cu^{+}, and as complexing agents for Cu^{2+} [19,20]. Interestingly, stoichiometric levels of RSH have been observed to *halt* copper-ion catalyzed RSNO decomposition, perhaps because of Cu^{2+} complexation by the corresponding thiolate (RS^{-}) [19,20]. While extensive work done on copper-ion catalyzed RSNO conversion to NO has resulted in valuable insights [18–24], even just the complete, balanced reaction stoichiometry for copper-ion catalyzed RSNO decomposition has not been experimentally determined, neither in the presence nor absence of added RSH. Of course, determination of the true reaction stoichiometry under the actual reaction conditions is *the necessary starting point* for any rigorous mechanistic study because the proposed mechanistic steps must, in turn, sum to the experimentally determined reaction stoichiometry. Without the true stoichiometry, one runs the risk of reporting the "mechanism" for a different reaction than is actually being investigated.

Due to the potentially toxic nature of freely diffusing copper ions in vitro, incorporation of copper ions into a solid support material for biomedical applications is desired [25–28]. Copper containing metal-organic frameworks (MOFs) are a class of porous solid materials containing organic linkers and copper cations that have been used to catalyze NO release from RSNO precursors [12,13]. The two copper based MOFs previously used in this regard are copper (II) benzene-1,3,5-tricarboxylate (Cu-BTC), and $H_3[(Cu_4Cl)_3\text{-}(BTTri)_8$, H_3BTTri = 1,3,5-tris (1*H*-1,2,3-triazol-5-yl) benzene] (CuBTTri), Fig. 1. Of these two, CuBTTri is attractive for incorporation into biomedical devices such as stents, catheters, and extracorporeal circuitry [29] because of its hydrothermal stability, its ability to catalyze GSNO decomposition in aqueous solutions [13,26], and because CuBTTri materials are compatible with human hepatocytes [30].

Important prior work is available testing CuBTTri as a catalyst material for endogenous NO generation [13,16,30]. Although CuBTTri

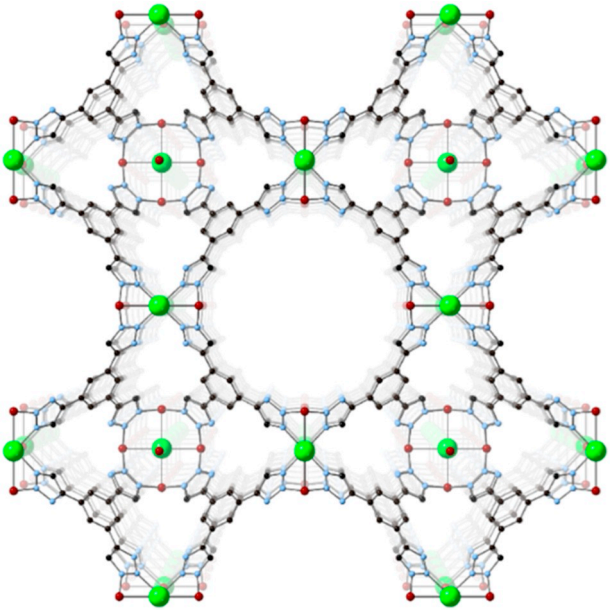

Fig. 1. One plausible CuBTTri subunit structure [42]. Shown are carbon (black), nitrogen (blue), chlorine (green), and copper (red). The open channels formed in CuBTTri may allow for diffusion of GSNO substrate into MOF pores via the largest, central channel. Open copper sites both at the surface and inside the CuBTTri pores are the plausible, expected active sites for GSNO binding and catalysis for NO release (specific coordination environments shown in Fig. S22).

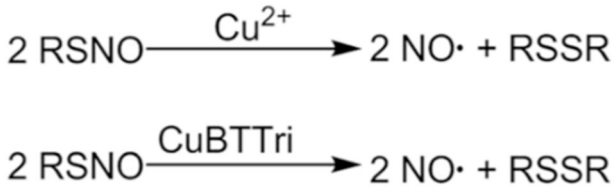

Scheme 1. Literature [13–15,24–27] idealized stoichiometry for copper catalyzed decomposition of GSNO.

catalyzed decomposition of GSNO is known to produce NO, the formation of glutathione disulfide (GSSG) has not yet been experimentally confirmed—nor has the complete reaction stoichiometry been experimentally determined for any copper MOF system. Additionally, the effect(s) and fate of added glutathione (GSH) in the CuBTTri MOF-catalyzed NO release reaction have not been explored, an important point given the apparent importance of thiols to the copper-ion system.

The reason these basic pieces of information about copper MOF systems and their NOR release catalysis are missing is because no method enabling the *simultaneous, direct monitoring* of [GSNO], [GSH], and [GSSG] *in water* has been reported [31]. The previously proposed stoichiometry [13–15,23–27] for both systems, Scheme 1, is widely accepted, *but has actually never been experimentally verified*. RSNO decomposition catalyzed by solvated copper ions and CuBTTri have been traditionally studied via either ultraviolet-visible (UV-VIS) spectroscopy (via the intensity of a peak at 335 nm caused by a $\pi \rightarrow \pi^{*}$ transition in the S—N bond of the RSNO) or nitric oxide analyzers (NOAs) [12,13] to track NO release [32,33]. NOA experiments use chemiluminescence to quantify the amount of gaseous NO generated [34]. NOAs and UV–visible monitor only the concentration of one chemical species in the complex reaction mixture and hence, are unable to determine the true, balanced reaction stoichiometry. Specifically, the amount of GSSG formed per amount of GSNO decomposed has never been previously determined in either the CuBTTri or the copper-ion system—and we demonstrate herein that the prior, assumed stoichiometry in Scheme 1 is not precisely correct. This in turn means that the prior mechanistic details for RSNO conversion to NO and the other products of the reaction cannot be exactly correct.

Herein, we report that solvent-suppressed ^{1}H nuclear magnetic resonance (^{1}H NMR) spectroscopy provides the needed ability to monitor GSNO decomposition catalyzed by either copper ion or CuBTTri in the blood-and hence biomedical applications-relevant solvent, *water*. Direct, simultaneous, and reliable quantification of [GSNO], [GSH], and [GSSG] in water is reported for the first time. Hydrogen bonding of RSNOs to water may, for example, account for part of RSNO in vivo stability [35,36]. We also compare copper-ion vs CuBTTri catalyzed release of NO from GSNO, an important [37] comparison by our direct ^{1}H NMR methodology given that copper ions are currently the most efficient copper pre-catalyst for NO release from GSNO [12,13,28].

2. Materials and methods

2.1. Reagents

Diethylamine (99%), trimethylsilylacetylene (98%), trimethylsilylazide (94%), and 1,3,5-tribromobenzene (98%) were purchased from Alfa Aesar (Ward Hill, MA, USA). Glutathione (98%) was purchased from VWR (Radnor, PA, USA). Sodium nitrite (99.5%), oxidized glutathione (98%), copper (I) iodide (99.5%), bis(triphenylphosphine) palladium(II) dichloride (99%), and dichloromethane (99%) were purchased from Sigma-Aldrich (St. Louis, MO, USA). HCl (1 N), methanol (99%), and sodium hydroxide (98.9%) were purchased from Fisher Scientific (Hampton, NH, USA). Dimethylformamide (99%) and copper (II) chloride dihydrate (99%) were purchased from EMD Chemicals (Gibbstown, NJ, USA). Ultrahigh purity nitrogen gas was

supplied by Airgas (Denver, CO, USA). Deionized water (18.2 MΩ·cm) was obtained from a Millipore Direct-Q water purification system (EMD Millipore, Billerica, MA, USA). All materials were used as received without any further purification.

2.2. Water suppression ^{1}H NMR methodology

All NMR experiments were performed using an Agilent Inova 500 equipped with a 5 mm pulsed-field-gradient HCN probe. Samples were prepared in septa-capped Wilmad 528-PP 500 MHz tubes under inert conditions (N_2). For this, 0.5 mL of reaction supernatant was added into an NMR tube containing 0.1 mL of 20 mM NaH_2PO_4 buffered D_2O and mixed by hand, followed by 2 s of sonication to remove any air bubbles. Samples were kept dark, air-free, and analyzed as soon as possible. NMR experiments were run using PRESAT with PURGE solvent signal suppression available in VnmrJ version-4.2 [50]. The system was buffered with NaH_2PO_4 to a pH of 4 due to the sensitivity of the compounds of interest (GSNO, GSH, GSSG) to the pH of the solvent. 512 transients were acquired for all samples, which took 35 min to complete. A 2 s square presat with a bandwidth of 100 Hz on resonance at 4.67 ppm (water) was used, followed by the PURGE crusher sequence and a pi/2 excitation pulse of 5.7 μs. Acquisition time was 2 s, so with the PRESAT delay the total time between transients was about 4 s.

2.3. GSNO synthesis

GSNO was prepared following an established literature protocol [51]. In brief: a solution of glutathione (1.53 g, 4.99 mmol) was prepared in Millipore filtered water (8 mL) containing 2 M HCl (2.5 mL). One equivalent of sodium nitrite (0.345 g, 4.99 mmol) was added and the resulting mixture was stirred for 40 min at 5 °C. Acetone (10 mL) was added to the resulting red solution and the mixture was stirred for another 10 min. The red precipitate was collected via vacuum filtration and washed with ice-cold water (5 × 5 mL) and ice-cold acetone (3 × 10 mL). The precipitate was then dried on a high vacuum line for 4 h to afford *S*-Nitrosoglutathione (1.31 g, 3.86 mmol, 77%) (λ_{max}) (H2O) 335, 550 nm (ε = 922, 15.9 cm^{-1} mM^{-1}). The GSNO sample used herein was determined to be 97 ± 2% pure (Table S4 and Fig. S5). This will prove important because even a 3 ± 2% GSH impurity from GSNO is potentially capable of initiating copper catalyzed NO release from GSNO.

2.4. H_3BTTri ligand synthesis

The H_3BTTri ligand was prepared following an established literature protocol [42]. In brief: solid 1,3,5-tribromobenzene (9.45 g, 30.0 mmol) was dissolved in diethylamine (250 mL) under inert conditions (N_2). Copper(I) iodide (50 mg, 0.26 mmol) and dichlorobis(triphenylphosphine)palladium(II) (400 mg, 0.57 mmol) were added to the stirred solution. Trimethylsilylacetylene (10.6 g, 108. mmol) was added to the solution and the resulting mixture was heated at 50 °C for 6 h. Resulting diethylamine hydrobromide was removed by filtration and washed with ether (45 mL). Combined washings were evaporated to dryness in vacuo and the resulting product purified by a silica plug to yield 9.61 g (78%) 1,3,5-tris(trimethylsilylethynyl)benzene as an intermediate. ^{1}H NMR (400 MHz, $CDCl_3$): δ = 7.43 (s), 0.23 (s) ppm.

The 1,3,5-tris(trimethylsilylethynyl)benzene intermediate (9.61 g, 26.3 mmol) was hydrolyzed by treatment with NaOH(aq) (30 mL, 1 M), CH_2Cl_2 (20 mL), and methanol (50 mL) via stirring at room temperature for 3 h. Work-up involving the evaporation of methanol, ether extraction of the residue, and evaporation of the solvent in vacuo yielded 2.68 g of white powder containing 1,3,5-triethynylbenzene. ^{1}H NMR (400 MHz, $CDCl_3$): δ = 7.51 (s), 3.12 (s) ppm.

Trimethylsilylazide (9.26 g, 80.4 mmol) was added to a solution of copper(I) iodide (510 mg, 2.63 mmol) and 1,3,5-triethynylbenzene (2.68 g, 17.8 mmol) under inert conditions in a mixture of dimethylformamide (DMF; 90 mL) and methanol (10 mL). The resulting mixture was stirred at 100 °C for 36 h. The mixture was then filtered and reduced to a volume of 10 mL via rotary evaporation. A pale-yellow precipitate was formed upon the addition of Millipore filtered water (30 mL) to the resulting filtrate. The solid was collected by filtration, washed with ether and dried in vacuo to yield 4.1 g (83%) of the product. ^{1}H NMR (400 MHz, $(CD_3)_2SO$): δ = 8.52 (s), 8.34 (s) ppm.

2.5. CuBTTri choice and synthesis

Choosing a MOF catalyst required careful consideration, as many MOF species are not stable in water or biological media [39–41]. Hence, CuBTTri was used based on prior evidence that the MOF is stable in both water and biological media [30,42]. CuBTTri was synthesized following a previously reported procedure [42]. A solution of H_3BTTri (225 mg, 0.937 mmol) in DMF (40 mL) was prepared in a 250 mL Pyrex bottle $CuCl_2{\cdot}2H_2O$ (383 mg, 2.25 mmol) was added to the solution. The vial was heated at 100 °C for 72 h to afford $H_3[(Cu_4Cl)_3(BTTri)_8(DMF)_{12}]{\cdot}7DMF{\cdot}76H_2O$. The purple powder was washed with boiling DMF (10 × 10 mL) and allowed to dry under ambient conditions to yield 218 mg (76%) of product. Solvent exchange via Soxhlet was performed using Millipore filtered water to yield $H_3[(Cu_4Cl)_3(BTTri)_8(DMF)_{12}]{\cdot}72H_2O$.

2.6. Reaction setup

All reactions described herein were carried out under inert, N_2 gas, atmosphere, unless otherwise noted. GSNO and GSH solutions were prepared from Millipore H_2O and solid GSNO or GSH powder under inert conditions (N_2) in a 200 mL round bottom flask. CuBTTri was weighed into a multi neck 100 mL round-bottomed flask and oven dried overnight at 110 °C. Following drying, the flask containing CuBTTri was placed under vacuum for 1 h on a Schlenk line and backfilled with N_2 (g) prior to reaction. GSNO and GSH solutions were then injected into the reaction flasks containing dry CuBTTri. Vigorous bubbling in the solution was established. Reaction flasks were wrapped in aluminum foil to prevent exposure to light and reactions proceeded for a predetermined time. To quench the reaction once the reaction time had been reached, the exit needle was removed to stop bubbling and the supernatant was carefully decanted via a syringe, leaving the MOF particles in the flask. The quenched reaction solution was then kept cool and dark in a Cu-free glass vial under inert conditions (N_2) or added directly to an NMR tube. The ^{1}H NMR sample was prepared in a septa capped sample tube under inert conditions (N_2) by injecting 0.5 mL of reaction supernatant into the NMR tube along with 0.1 mL of 20 mM NaH_2PO_4 buffered D_2O. An identical procedure as described was carried out for the reaction between GSNO and $CuCl_2$. No unanticipated safety hazards were encountered over the course of all experiments. All reactions reported in the Results and discussion section of this work were performed in triplicate to obtain an average and standard deviation.

2.7. ^{1}H NMR

All free induction decay (FID) spectra were processed using MestraNova® software to examine peak intensities and integration values. Data analysis and calculations were performed using Microsoft Excel®.

2.8. Nitric oxide analyzer (NOA) detection of NO

Control experiments were performed for both the copper-ion and CuBTTri catalysis systems to confirm that the previously observed release of 1 mol NO/mol GSNO [12,13] does in fact occur and is detectable in our hands for both catalyst systems. The details and results are provided in Figs. S18–S21 of the Supporting information. These

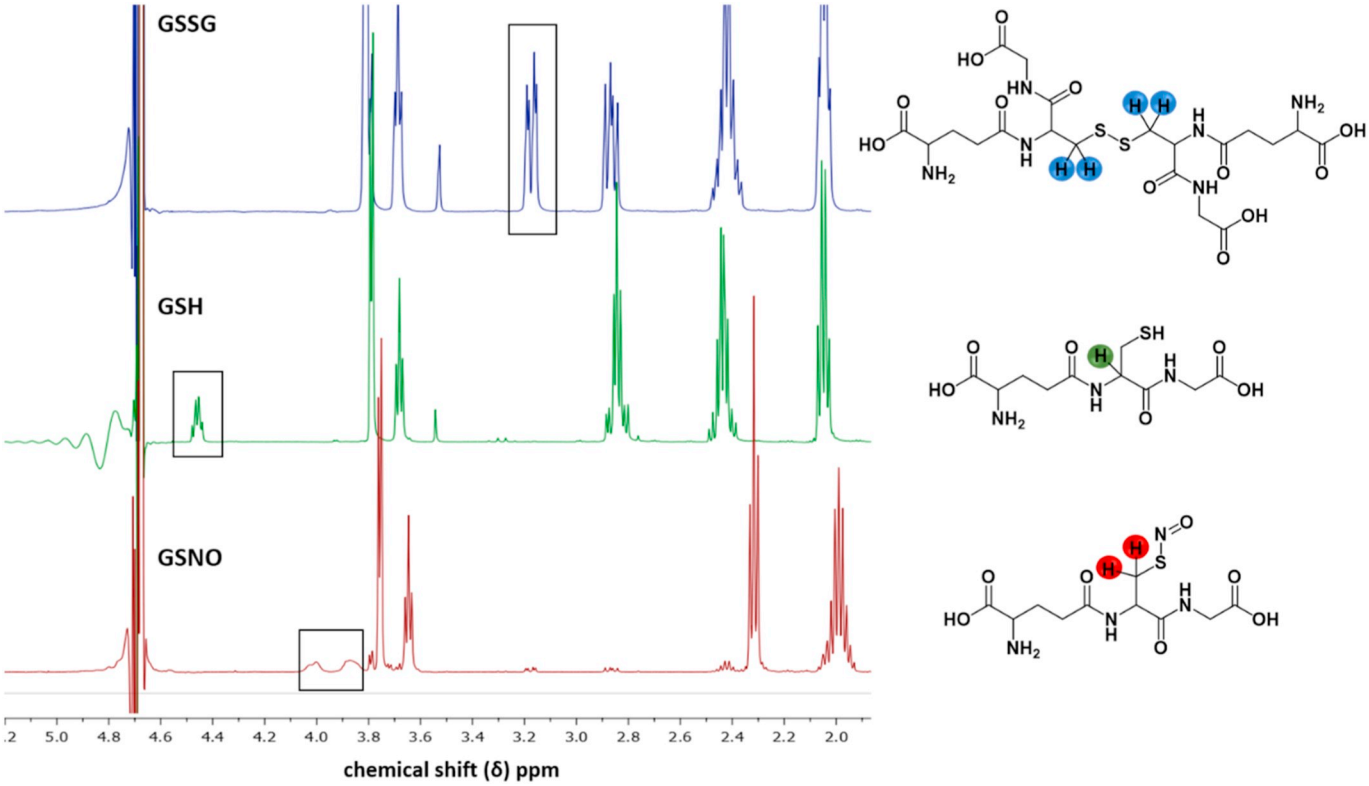

Fig. 2. Structures and diagnostic peaks used for ^{1}H NMR analysis of GSSG (blue, top), GSH (green, middle), and GSNO (red, bottom) in 0.5 mL H_2O and 0.1 mL 20 mM NaH_2PO_4 buffered D_2O.

reactions were performed under identical conditions to those described above in the Reaction setup subsection of the Materials and methods section (vide supra).

3. Results and discussion

3.1. ^{1}H NMR of the individual reaction components

Despite their structural similarities, each individual reaction component, GSNO, GSH, and GSSG, proved to contain distinguishable ^{1}H NMR signals, in 20 mM NaH_2PO_4 buffered 90% H_2O 10% D_2O, Fig. 2. Specifically, GSSG displays two doublets of doublets at 3.15–3.19 ppm and 2.84–2.89 ppm identified as the protons on the carbon adjacent to the sulfur groups. GSH displays a multiplet at 4.40–4.48 ppm associated with the C—H two carbons away from the sulfur group and a multiplet at 2.80–2.88 ppm attributed to the protons adjacent to the sulfur group. The two protons on the carbon adjacent to the sulfur group in GSNO appear as two distinctly broad peaks at 4.00–4.03 ppm and 3.85–3.89 ppm. All individual peaks that were used for determining the concentration of reaction components are identified with boxes in Fig. 2.

Initial attempts to determine reaction species concentration used benzene as an internal quantitative standard, but the significant difference in longitudinal relaxation time, T_1, among various reaction components and benzene protons afforded a large error under the conditions necessary for data acquisition. In response, efforts were directed to quantify the individual reaction components in solution directly by developing an absolute calibration curve based on known concentrations of authentic GSNO, GSH, and GSSG. The intensity of the signals used to quantify GSNO and GSH were affected by the solvent suppression method due to their proximity to the water peak. However, the magnitude of this effect was stable and consistent from experiment-to-experiment over a concentration range from 500 μM to 3 mM. Hence, the necessary calibration curves were generated using 4 different concentrations for each component (500 μM, 1 mM, 2 mM, and 3 mM). A calibration curve was constructed whereby the intensity of the highest peak within the boxed regions shown in Fig. 2 was plotted on the y-axis and concentration plotted on the x-axis (Figs. S8–S10). A linear fit was applied yielding the following equations where y is signal intensity and x is species concentration (in mmol/L), all fits having R^2 values > 0.99:

$$[\text{GSNO}]: \quad y = 28.4x - 2.05 \tag{1a}$$

$$[\text{GSH}]: \quad y = 138x - 17.5 \tag{1b}$$

$$[\text{GSSG}]: \quad y = 368x + 223 \tag{1c}$$

Buffering the system with NaH_2PO_4 for NMR analysis was critical to prevent peak broadening and unwanted competing reaction pathways that could arise from minor differences in pH. DMSO was also examined as a possible solvent, but proved inferior to water as it either prevented any decomposition or yielded unwanted oxidization of GSH to GSSG [38]. In short, a direct method has been developed that allows the quantitative analysis of the reactions of CuBTTri and Cu^{2+} with the biologically relevant GSNO, *all in water* as a preferred solvent, and which can simultaneously detect each of the reactions' starting material and products (other than NO, which is detected separately, vide infra) GSNO, GSH, and GSSG.

3.2. Cu^{2+} pre-catalyst GSNO decomposition, first without added GSH

With a reliable, quantitative ^{1}H NMR technique to monitor [GSNO], [GSH], and [GSSG], the ostensibly simplest, solvated copper-ion catalyzed decomposition of GSNO was investigated first, under N_2 (g). Entry 2 in Table 1 summarizes the results of the reaction between GSNO (1 mM) and Cu^{2+} (0.2 mM) in water over 16 h *with no added GSH*. Complete decomposition of GSNO was observed within 16 h, as shown in Fig. 3. The only detectable products by ^{1}H NMR from the conversion of GSNO are GSSG and what matches a GSSG-Cu^{2+} chelate complex

Table 1
Concentration values (expressed in mmol/L) for reactants and products in the Cu^{2+} catalyzed system initially at 0 h and then after 16 h. All values at 16 h represent the average of three trials with standard deviation.

Entry	Initial conditions, T = 0 h				T = 16 h				
	$[GSH]_{Added}$	[GSNO]	$[Cu^{2+}]$	[NO]	[GSH]	[GSNO]	$[GSSG]_{Total}$	[NO] (Figs. S18, S20, S21)	% GSNO decomposition
1	0.04	1.0	0	0	N/A	1.0 ± 0.01	0 ± 0.05	0	0
2	0	1.0	0.2	0	N/A	0	0.5 ± 0.1	1.0 ± 0.1	100
3	0.04	1.0	1.0	0	N/A	0	0.4 ± 0.1	1.0 ± 0.1	100
4	1.0	1.0	0.2	0	1.0	0.75 ± 0.1	0.2 ± 0.1	0.25 ± 0.1	25

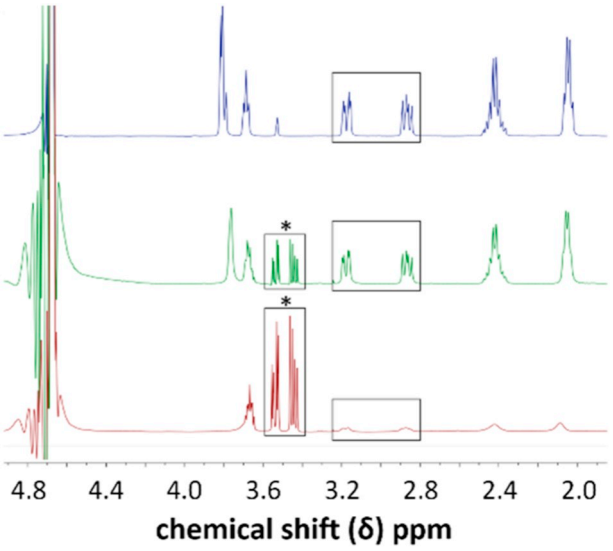

Fig. 3. Top, blue: GSSG (2 mM) in H_2O. Decomposition of GSNO (1 mM) with Cu^{2+} (0.2 mM, middle, green) (1 mM, bottom, red) in H_2O over 16 h. * indicates a GSSG-Cu^{2+} complex.

(also previously reported in the literature by Noble et al., Kenche et al., and Gorren et al. [20,43,44]), shown in boxes in Fig. 3, right and left, respectively.

The amount of GSSG formed was quantified using the previously described calibration curves, while the concentration of the chelate complex was determined via the relative peak integrations between the GSSG signal and the GSSG-Cu^{2+} complex signal. Together, these two concentrations sum to $[GSSG]_{Total}$, which in turn is equal to half of the initial [GSNO] within experimental error, as expected based on mass balance. The chelate complex exhibits the same splitting pattern as GSSG, with shifts further downfield (3.40–3.58 ppm) upon chelation of GSSG to Cu^{2+} ions, Fig. 3. Furthermore, formation of a GSSG-Cu^{2+} chelate complex is supported by the observation that as the initial $[Cu^{2+}]$ is increased, the relative concentration of the chelate complex increases rather than GSSG, as shown by the red trace in Fig. 3. The net reaction stoichiometry is shown in Scheme 2:

Of note here is that the ^{1}H NMR demonstrated stoichiometry in Scheme 2 deviates from the previously hypothesized, idealized stoichiometry, Scheme 1, in that 25% of the "RS·" by-product of NO release from GSNO winds up as GSSG-Cu^{2+}, that is, GSSG bound to Cu^{2+}. Overall, the observed reaction stoichiometry in Scheme 2 is the first time the amount of GSSG and GSSG-Cu^{2+} formed have been quantified for copper-ion catalyzed GSNO decomposition towards release of NO.

$$0.25\ Cu^{2+} + 2\ GSNO \xrightarrow{Cu^{2+}} 2\ NO^{\cdot} + 0.75\ GSSG + 0.25\ [GSSG\text{-}Cu^{2+}]$$

Scheme 2. Reaction stoichiometry for Cu^{2+} (0.2 mM) catalyzed release of NO from GSNO (1 mM) *without added GSH*.

3.3. Cu^{2+} pre-catalyst GSNO release of NO, with added GSH

The GSNO sample used herein is determined to be 97 ± 2% pure by UV-VIS spectroscopy (Table S4, Fig. S5). However, the literature suggests [20] that small (< 5%) impurity of GSH present in all GSNO samples (leftover from the synthesis) could be sufficient to initiate the reaction via reduction of Cu^{2+} to Cu^{+} [20]. Hence, this small GSH impurity could be critical to NO release catalysis, at least for the case of Cu^{2+}.

To probe the possible importance of GSH on the reaction, NO release from GSNO under Cu^{2+} pre-catalyst conditions was probed with 0.04 and then 1.0 equivalents of added GSH per equivalent of GSNO. The results are given in Table 1 entries 3 and 4, and Schemes 3 and 4. A control showing no GSNO conversion over 16 h if Cu^{2+} is omitted (and with 0.04 equivalents GSH added) is summarized in Entry 1 of Table 1 and the resulting ^{1}H NMR is shown in Fig. S13. The addition of sub-stoichiometric levels of GSH (1:5 ratio of $[GSH]:[Cu^{2+}]$) did not prevent the reaction from reaching completion within 16 h (Entry 3, Table 1), in agreement with previous reports [19,20]. The only products detectable by ^{1}H NMR are GSSG and the GSSG-Cu^{2+} chelate complex, as shown in Fig. 4. The total concentration of GSSG containing species is equal to half of the initial [GSNO] within experimental error, as summarized in the stoichiometry reported in Scheme 3.

On the other hand, the introduction of stoichiometric GSH (vs the amount of GSNO) to the reaction system, resulting in a 5:1 ratio of $[GSH]:[Cu^{2+}]$, led to an incomplete reaction after 16 h (Fig. S16). Excess GSH has previously been reported to halt GSNO decomposition, potentially via competitive complexation of Cu^{2+} and/or Cu^{+} ions by the carboxylate or thiolate of GSH, rendering the ions inactive for GSNO decomposition, Table 1, Entry 4 (Scheme 4) [18–20,43,45]. NOA experiments carried out under these same conditions also show an incomplete reaction (Fig. S20). Our direct ^{1}H NMR- determined results on Cu^{2+} catalysis at various [GSH] are, then, fully consistent with the prior literature in that sub-stoichiometric (0.04 mM) levels of GSH do not poison Cu^{2+} catalysis while stoichiometric (1 mM) levels do [18–24].

3.4. CuBTTri pre-catalyst GSNO to NO conversion catalysis, first without added GSH

Next, the CuBTTri catalyzed release of NO from GSNO was examined by ^{1}H NMR, first with no added GSH. All experiments were carried out with a 2:1 ratio of GSNO-to-copper centers in the MOF. Reaction supernatant and MOF samples used for the experiments were

$$0.25\ Cu^{2+} + 2\ GSNO \xrightarrow{Cu^{2+},\ GSH} 2\ NO^{\cdot} + 0.75\ GSSG + 0.25\ [GSSG\text{-}Cu^{2+}]$$

Scheme 3. Observed stoichiometry for Cu^{2+} (0.2 mM) catalyzed release of NO from GSNO (1 mM) with added sub stoichiometric GSH (0.04 mM).

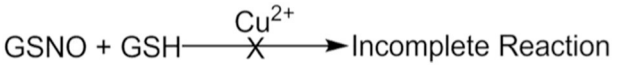

Scheme 4. Observed, incomplete reaction between Cu^{2+} (0.2 mM) and GSNO (1 mM) with added *stoichiometric* GSH (1 mM).

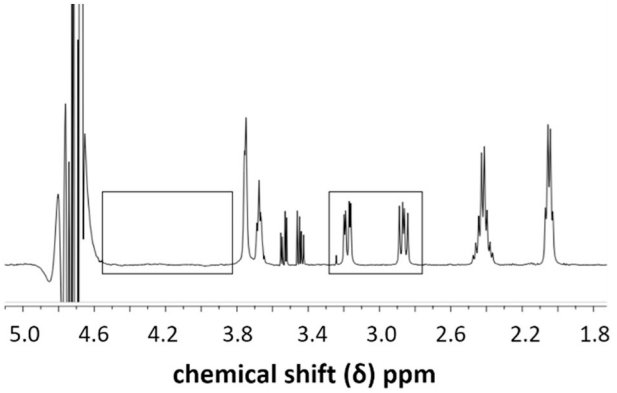

Fig. 4. GSNO (1 mM) reaction in the presence of Cu^{2+} ions (0.2 mM) and GSH (0.04 mM) in H_2O after 16 h.

saved to test for framework stability over the course of the reaction.

Fig. 5 depicts a ^1H NMR spectrum of the reaction between CuBTTri and GSNO (2 mM) in water taken at 16 h where the boxed peaks correspond to the unreacted GSNO on the left and GSSG product on the right. Entry 1 in Table 2 summarizes the results of the reaction after 16 h: the system did not reach completion, and instead resulted in only 10% GSNO decomposition. The resulting GSNO conversion stoichiometry is shown in Scheme 5.

Clearly the low level of GSH inherently present in the GSNO samples is insufficient to activate CuBTTri for complete GSNO decomposition. This result is quite different than the reactions with Cu^{2+} ions, that went to 100% completion under analogous conditions (vide supra). Given the literature hypothesis [18] that Cu^{+} is necessary for copper-ion catalyzed GSNO decomposition, it seemed prudent to introduce additional GSH in an attempt to activate the MOF pre-catalyst for GSNO decomposition, so those experiments were performed next.

3.5. CuBTTri catalyzed GSNO to NO conversion, with added GSH

The next system examined was a CuBTTri catalyzed reaction in which a stoichiometric equivalent of GSH (2 mM) was added to a reaction mixture containing GSNO (2 mM) and CuBTTri in water, then examined after 16 h. Complete GSNO decomposition is observed within 16 h and GSSG is the only product detectable by ^1H NMR, Fig. 6. One equivalent of GSSG is formed per 2 equivalents of GSNO decomposed.

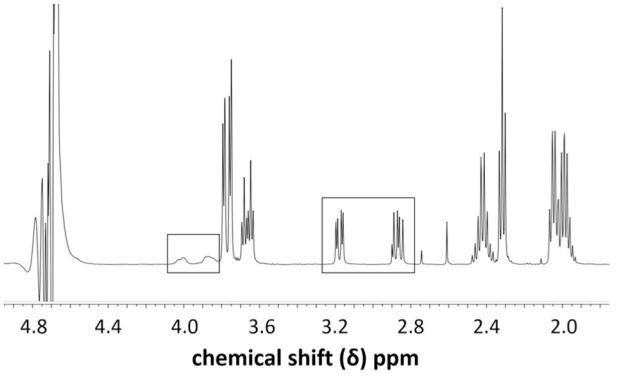

Fig. 5. GSNO (2 mM) conversion after 16 h in the presence of CuBTTri in H_2O at a ratio of 2:1 mol GSNO:mol Cu atoms in the MOF sample.

The resultant stoichiometry is reported in Scheme 6, and the overall tabulated results are provided in Entry 2 of Table 2.

Of considerable interest in the CuBTTri catalyzed reaction, and vs its Cu^{2+} ion counterpart, is that *complete GSNO decomposition is observed* even in the presence of stoichiometric GSH over 16 h. That is, unlike copper ions, *the active sites in CuBTTri are not deactivated by the introduction of stoichiometric GSH*. Moreover, the requirement for GSH is sub stoichiometric in the CuBTTri system, only 15% of the added 1.0 equivalent (0.3 equivalents in Scheme 6 vs 2 GSNO) being consumed at the end of the full GSNO conversion and NO release reaction. Leftover GSH is shown in Fig. 6 in the left-most box. A control experiment with no CuBTTri present was performed to ensure that observed reactivity was not solely induced by GSH [46,47]. No reaction within experimental error between GSNO (2 mM) and GSH (2 mM) over 14 h is observed in the absence of CuBTTri (Fig. S14) supporting the hypothesis that CuBTTri is a necessary pre-catalyst, along with the GSH.

The sub-stoichiometric GSH requirement again looks to be involved in the activation of the Cu catalyst (in this case CuBTTri), since entry 1 of Table 2 shows only 10% reaction in the absence of added GSH. Indeed, one hypothesis is that the 0.3 GSH is activating (reducing, hence "titrating") a 0.3 fraction of Cu sites in the CuBTTri pre-catalyst (Fig. 1, vide supra). Scheme 6 is written to reflect this hypothesis, specifically presently as "[(0.3GSH)-CuBTTri]" which is meant to convey only the net composition of this complex. Further studies on the number and type of active sites in the CuBTTri are warranted and in progress. Note also, once again, that the true stoichiometry in Scheme 6—and by necessity the underlying reactions that add up to this stoichiometry and, hence, the overall mechanism—are different than the prior literature's stoichiometry for RSNO conversion, Scheme 1 (vide supra). Once again, the value of the presented direct ^1H NMR monitoring method for RSNO conversion in water is apparent.

3.6. Evidence against copper-ion leaching from CuBTTri

Tests were performed to determine if copper ions were leaching from the CuBTTri under the reaction conditions. Specifically, inductively coupled plasma atomic emission spectroscopy (ICP-AES) analysis of the reaction supernatant after 16 h indicated that < 1% of the total copper from the MOF was in solution (Table S7). The lack of ≥1% copper in solution (≤~10^{-6} M Cu^{2+}) argues compellingly against GSNO conversion being catalyzed by Cu^{2+} ions released from the MOF. First, the [GSH]:[Cu^{2+}] ratio would be approximately 1000:1 and we have shown herein that even a 1:1 ratio poisons copper-ion catalysis, results consistent with the finding of others [19]. Furthermore, no GSSG-Cu^{2+} complex is observed for incomplete or completed CuBTTri reactions (Figs. 5 and 6), further discrediting significant leaching of copper atoms from the framework. The MOF also retains crystallinity over the course of the reaction as verified by powder X-ray diffraction (pXRD) data (Fig. S17). In short, the "leached Cu^{2+} is the catalyst" hypothesis for the CuBTTri MOF is disproven (consistent with previous studies reported by our group) [12,13].

4. Conclusions

The following are the key findings of the present studies:

(1) ^1H NMR with solvent suppression proves to be a valuable, direct technique to track copper catalyzed release of NO from bio-available GSNO in water, thereby making the results herein relevant at least in principle to other, aqueous-based systems such as blood with its ~80% water content.
(2) The ^1H NMR method allows each of [GSNO], [GSH], and [GSSG] to be monitored simultaneously and directly by their differentiable ^1H NMR signals. This tracking in turn led to four balanced reaction stoichiometries not previously available, those for GSNO conversion with Cu^{2+} or CuBTTri pre-catalysts, each with and without

Table 2
Concentration values (expressed in mmol/L) for reactants and products in the CuBTTri catalyzed system initially at 0 h and then after 16 h. All values at 16 h represent the average of three trials with standard deviation.

Entry	Initial conditions, T = 0 h				T = 16 h				
	$[GSH]_{Added}$	[GSNO]	CuBTTri[a]	[NO]	[GSH]	[GSNO]	[GSSG]	[NO] (Fig. S19)	% GSNO decomposition
1	0	2.0	0.015	0	0	1.9 ± 0.1	0 ± 0.1	N/A	10
2	2.0	2.0	0.015	0	1.7 ± 0.1	0	0.9 ± 0.1	2.0 ± 0.1	100

[a] Value expressed in mmol. Due to the heterogeneous nature of the MOF pre-catalyst the appropriate mass was added to yield a 2:1 ratio of GSNO molecules to copper MOF atoms to achieve catalytic conditions.

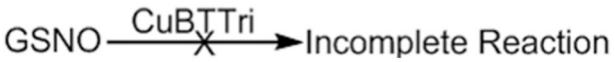

Scheme 5. Observed, incomplete reaction between GSNO (2 mM) and CuBTTri *without added GSH*.

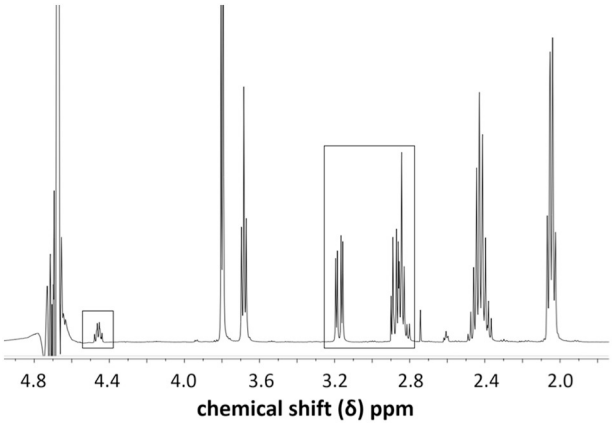

Fig. 6. Conversion of GSNO (2 mM) in the presence of GSH (2 mM) and CuBTTri in H_2O over 16 h with 2:1 mol GSNO:mol Cu in the MOF sample.

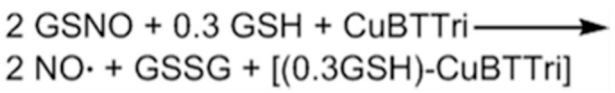

Scheme 6. Observed stoichiometry for CuBTTri catalyzed GSNO (2 mM) decomposition with added *stoichiometric* GSH (2 mM).

added GSH from sub-stoichiometric to stoichiometric levels, Schemes 2, 3, 5, and 6.

(3) Importantly, in 3 cases those reaction stoichiometries—and, hence, the underlying mechanism adding up to those net reactions—are distinct vs the literature's assumed, idealized stoichiometry, Scheme 1. The formation and quantification of GSSG-Cu^{2+}, and what we write compositionally as [(0.3GSH)-CuBTTri], are the primary differences vs what one finds in the literature.

(4) Significantly, copper-ion and CuBTTri catalyzed systems show key differences in reactivity towards the amount of GSH present initially: sub-stoichiometric levels of GSH are sufficient for 100% GSNO conversion by copper ions (Table 1, entries 2 and 3), but allow only 10% conversion of GSNO using CuBTTri (Table 2, entry 1). In stark contrast, when 1.0 equivalent of GSH is added only 25% GSNO conversion is seen using Cu^{2+} (Table 1, entry 4) while 100% GSNO conversion to NO is achieved by CuBTTri (Table 2, entry 2). The results between the two pre-catalysts are essentially completely flipped by the absence or presence of more than trace GSH. These observations support computational studies by Kumar et al. suggesting that RSH species can interact with coordinatively unsaturated copper centers in MOFs to activate them for RSNO decomposition [48,49].

(5) Critically, taken together, the above findings lead to the inescapable conclusion that the copper-ion and CuBTTri catalyzed reactions *must be operating through different mechanistic pathways*. The Cu^{2+} precatalyst operates at a greater catalytic rate, the CuBTTri and Cu^{2+} exhibit inverse responses to the addition of stoichiometric and sub-stoichiometric GSH, and the reaction products of the two systems differ. Further investigation into why and how those mechanisms differ is a goal of our ongoing studies.

(6) Lastly, with the ^{1}H NMR methodology developed herein, kinetic and mechanistic studies of copper catalyzed GSNO release of NO become possible and can be based on a direct method. The comparison of the Cu^{2+} and CuBTTri based pathways promises to be an interesting comparison. Determining the number and type of active sites in the CuBTTri system is another important goal, with efforts in progress. Finally, application of the ^{1}H NMR method to reactions carried out in blood/biological milieu is another important future goal, one made eventually possible by the present study in water emphasizing the bio-available substrate, GSNO, and its complete reaction products upon the desired release of NO for medically important applications.

Declaration of Competing Interest

The authors declare the following competing financial interest(s): Prof. Melissa M. Reynolds is an equity holder in Diazamed, Inc. which has exclusively licensed the MOF platform from CSU Ventures. The other authors have no competing interests.

Acknowledgements

The authors thank Jim Self-and Debbie Weddle in the CSU Soil, Water and Plant Testing Lab for ICP-AES analysis. This work was supported by an NSF Career Award, #1352201, NSF Grant #1664646, NIH grant #1S10OD021814-01, and NIH grant #1R01HL140301-02.

Appendix A. Supplementary data

Supplementary data to this article can be found online at https://doi.org/10.1016/j.jinorgbio.2019.110760.

References

[1] Roy, B.; du Moulinet d'Hardemare, A.; Fontecave, M. New thionitrites: synthesis, stability, and nitric oxide generation. J. Org. Chem. 1994, 59, 7019.
[2] D.R. Williams, M.-R. Lee, Y.-A. Song, S.-K. Ko, G.-H. Kim, I. Shin, Synthetic small molecules that induce neurogenesis in skeletal muscle, J. Am. Chem. Soc. 129 (2007) 9258.
[3] A.B. Knott, E. Bossy-Wetzel, Nitric oxide in health and disease of the nervous system, Antioxid. & Redox Sign 11 (2009) 541.
[4] C. Bogdan, Nitric oxide and the immune response, Nat. Immunol. 2 (2001) 907.
[5] J.W. Coleman, Nitrix oxide in immunity and INflammation, Int. Immunopharmacol. 1 (2001) 1397.
[6] R.M.J. Palmer, A.G. Ferrige, S. Moncada, Nitric oxide release accounts for the biological activity of endothelium-derived relaxing factor, Nature 327 (1987) 524.
[7] M.A. Marletta, Nitrix oxide: biosynthesis and biological significance, Trends Biochem. Sci. 14 (1989) 488.
[8] A.W. Carpenter, M.H. Schoenfisch, Nitric oxide release: part II. Therapeutic

applications, Chem. Soc. Rev. 41 (2012) 3742.
[9] D.O. Schairer, J.S. Chouake, J.D. Nosanchuk, A.J. Friedman, The potential of nitric oxide releasing therapies as antimicrobial agents, Virulence 3 (2012) 271.
[10] D. Tsikas, M. Schmidt, A. Böhmer, A.A. Zoerner, F.-M. Gutzki, J. Jordan, UPLC-MS/MS measurement of *S*-nitrosoglutathione (GSNO) in human plasma solves the *S*-nitrosothiol concentration enigma, J. Chromatogr. B 927 (2013) 147.
[11] D. Tsikas, E. Hanff, A. Mengel, C. Lindermayr (Eds.), Nitric Oxide: Methods and Protocols, Springer New York, New York, NY, 2018, p. 113.
[12] J.L. Harding, M.M. Reynolds, Metal organic frameworks as nitric oxide catalysts, J. Am. Chem. Soc. 134 (2012) 3330.
[13] Jacqueline, L. Harding, Jarid, M. Metz, Reynolds Melissa, M.A. Tunable, Stable, and bioactive MOF catalyst for generating a localized therapeutic from endogenous sources, Adv. Funct. Mat. 24 (2014) 7503.
[14] P.-T. Kao, I.J. Lee, I. Liau, C.-S. Yeh, Controllable NO release from $Cu_{1.6}S$ nanoparticle decomposition of *S*-nitrosoglutathiones following photothermal disintegration of polymersomes to elicit cerebral vasodilatory activity, Chem. Sci. 8 (2017) 291.
[15] H.A. Pal, S. Mohapatra, V. Gupta, S. Ghosh, S. Verma, Self-assembling soft structures for intracellular NO release and promotion of neurite outgrowth, Chem. Sci. 8 (2017) 6171.
[16] M.J. Neufeld, A. Lutzke, W.M. Jones, M.M. Reynolds, Nitric oxide generation from endogenous substrates using metal-organic frameworks: inclusion within poly(vinyl alcohol) membranes to investigate reactivity and therapeutic potential, ACS Appl. Mater. Interfaces 9 (2017) 35628.
[17] S.C. Askew, D.J. Barnett, J. McAninly, D.L.H. Williams, Catalysis by Cu^{2+} of nitrix oxide release from *S*-nitrosothiols (RSNO), J. Chem. Soc. Perk. T. 2 (1995) 741.
[18] A.P. Dicks, H.R. Swift, D.L.H. Williams, A.R. Butler, H.H. Al-Sa'doni, B.G. Cox, Identification of Cu^{+} as the effective reagent in nitric oxide formation from *S*-nitrosothiols (RSNO), J. Chem. Soc. Perk. T. 2 (1996) 481.
[19] P. Dicks, A.; Herves Beloso, P.; Lyn H. Williams, D. Decomposition of *S*-nitrosothiols: the effects of added thiols. J. Chem. Soc. Perk. T. 2 1997, 1429.
[20] A.C.F. Gorren, A. Schrammel, K. Schmidt, B. Mayer, Decomposition of *S*-nitrosoglutathione in the presence of copper ions and glutathione, Arch. Biochem. Biophys. 330 (1996) 219.
[21] S. Zhang, N. Çelebi-Ölçüm, M.M. Melzer, K.N. Houk, T.H. Warren, Copper(I) nitrosyls from reaction of copper(II) thiolates with *S*-nitrosothiols: mechanism of NO release from RSNOs at Cu, J. Am. Chem. Soc. 135 (2013) 16746.
[22] J.N. Smith, T.P. Dasgupta, Kinetics and mechanism of the decomposition of *S*-nitrosoglutathione by l-ascorbic acid and copper ions in aqueous solution to produce nitric oxide, Nitric Oxide 4 (2000) 57.
[23] A. Burg, H. Cohen, D. Meyerstein, The reaction mechanism of nitrosothiols with copper(I), J. Biol. Inorg. Chem. 5 (2000) 213.
[24] M.M. Melzer, S. Mossin, A.J.P. Cardenas, K.D. Williams, S. Zhang, K. Meyer, T.H. Warren, A copper(II) thiolate from reductive cleavage of an *S*-nitrosothiol, Inorg. Chem. 51 (2012) 8658.
[25] S.C. Luza, H.C. Speisky, Liver copper storage and transport during development: implications for cytotoxicity, Am. J. Clin. Nutr. 63 (1996) 812.
[26] M.J. Neufeld, A. Lutzke, J.B. Tapia, M.M. Reynolds, Metal-organic framework/chitosan hybrid materials promote nitric oxide release from *S*-nitrosoglutathione in aqueous solution, ACS Appl. Mater. Interfaces 9 (2017) 5139.
[27] H. Ren, J. Wu, C. Xi, N. Lehnert, T. Major, R.H. Bartlett, M.E. Meyerhoff, Electrochemically modulated nitric oxide (NO) releasing biomedical devices via copper(II)-tri(2-pyridylmethyl)amine mediated reduction of nitrite, ACS Appl.Mater. Interfaces 6 (2014) 3779.
[28] K. Liu, M.E. Meyerhoff, Preparation and characterization of an improved Cu^{2+}-cyclen polyurethane material that catalyzes generation of nitric oxide from *S*-nitrosothiols, J. Mater. Chem. 22 (2012) 18784.
[29] T.R.N. Roberts, J. Megan, Michael A. Meledeo, Andrew P. Cap, C. Cancio Leopoldo, Melissa M. Reynolds, Andriy I. Batchinsky, A metal organic framework reduces thrombus formation and platelet aggregation ex vivo, J. Trauma Acute Care 85 (2018) 572–579.
[30] M.J. Neufeld, B.R. Ware, A. Lutzke, S.R. Khetani, M.M. Reynolds, Water-stable metal-organic framework/polymer composites compatible with human hepatocytes, ACS Appl. Mater. Interfaces 8 (2016) 19343.
[31] A.R. Diers, A. Keszler, N. Hogg, Detection of *S*-nitrosothiols, Biochim. Biophys. Acta 1840 (2013) 892.
[32] D.L.H. Williams, The chemistry of *S*-nitrosothiols, Accounts Chem. Res. 32 (1999) 869.
[33] M.D. Bartberger, K.N. Houk, S.C. Powell, J.D. Mannion, K.Y. Lo, J.S. Stamler, E.J. Toone, Theory, spectroscopy, and crystallographic analysis of *S*-nitrosothiols: conformational distribution dictates spectroscopic behavior, J. Am. Chem. Soc. 122 (2000) 5889.
[34] Instruments, G. A. 2014.
[35] L.-S. Choi, H. Bayley, *S*-nitrosothiol chemistry at the single-molecule level, Angew. Chem. Int. Ed. 51 (2012) 7972.
[36] C. Baciu, K.-B. Cho, J.W. Gauld, Influence of Cu^{+} on the RS-NO bond dissociation energy of *S*-nitrosothiols, J. Phys. Chem. B 109 (2005) 1334.
[37] P. García-García, M. Müller, A. Corma, MOF catalysis in relation to their homogeneous counterparts and conventional solid catalysts, Chem. Sci. 5 (2014) 2979.
[38] N.Z.M. Homer, J. Reglinski, R. Sowden, C.M. Spickett, R. Wilson, J.J. Walker, Dimethylsulfoxide oxidizes glutathione in vitro and in human erythrocytes: kinetic analysis by ^{1}H NMR, Cryobiology 50 (2005) 317.
[39] L. Huang, H. Wang, J. Chen, Z. Wang, J. Sun, D. Zhao, Y. Yan, Synthesis, morphology control, and properties of porous metal-organic coordination polymers, Micropor. Mesopor. Mat. 58 (2003) 105.
[40] P.M. Schoenecker, C.G. Carson, H. Jasuja, C.J.J. Flemming, K.S. Walton, Effect of water adsorption on retention of structure and surface area of metal-organic frameworks, Ind. Eng. Chem. Res. 51 (2012) 6513.
[41] N. Al-Janabi, P. Hill, L. Torrente-Murciano, A. Garforth, P. Gorgojo, F. Siperstein, X. Fan, Mapping the Cu-BTC metal-organic framework (HKUST-1) stability envelope in the presence of water vapour for CO_2 adsorption from flue gases, Chem. Eng. J. 281 (2015) 669.
[42] A. Demessence, D.M. D'Alessandro, M.L. Foo, J.R. Long, Strong CO_2 binding in a water-stable, triazolate-bridged metal-organic framework functionalized with ethylenediamine, J. Am. Chem. Soc. 131 (2009) 8784.
[43] R. Noble, D., R. Swift, H., H. Lyn, D. Williams, Nitric oxide release from *S*-nitrosoglutathione, Chem. Commun. 2317 (1999).
[44] V.B. Kenche, I. Zawisza, C.L. Masters, W. Bal, K.J. Barnham, S.C. Drew, Mixed ligand Cu^{2+} complexes of a model therapeutic with Alzheimer's amyoid-β peptide and monoamine neurotransmitters, Inorg. Chem. 52 (2013) 4303.
[45] K.B.-M.C. Ngamchuea, R.G. Compton, The copper(II)-catalyzed oxidation of glutathione, Chem. Eur. J. 22 (2016) 15545.
[46] D. Pietraforte, C. Mallozzi, G. Scorza, M. Minetti, Role of thiols in the targeting of *S*-nitroso thiolsto red blood cells, Biochemistry 34 (1995) 7177.
[47] S.P. Singh, J.S. Wishnok, M. Keshive, W.M. Deen, S.R. Tannenbaum, The chemistry of the *S*-nitrosoglutathione/glutathione system, Proc. Natl. Acad. Sci. U. S. A. 93 (1996) 14428.
[48] K. Taylor-Edinbyrd, T. Li, R. Kumar, Effect of chemical structure of *S*-nitrosothiols on nitric oxide release mediated by the copper sites of a metal organic framework based environment, Phys. Chem. Chem. Phys. 19 (2017) 11947.
[49] T. Li, K. Taylor-Edinbyrd, R. Phys Kumar, A computational study of the effect of the metal organic framework environment on the release of chemically stored nitric oxide, Chem. Chem. Phys. 17 (2015) 23403.
[50] A.J. Simpson, S.A. Brown, Purge NMR: effective and easy solvent suppression, J. Magn. Reson. 175 (2005) 340.
[51] T.W. Hart, Some observations concerning the *S*-nitroso and *S*-phenylsulphonyl derivatives of L-cysteine and glutathione, Tetrahedron Lett. 26 (1985) 2013.